Analysis of Th and U breeding in a heat pipe cooled traveling wave reactor

Kunfeng Ma and Po Hu*

School of Nuclear Science and Engineering, Shanghai Jiao Tong University, Shanghai, China

Introduction: Heat pipe cooled traveling wave reactor (HPTWR) is a newly proposed heat pipe reactor. The HPTWR can achieve the low enrichment of loaded fuel, small reactivity swing, and long-term continuous operation for the power supply of decentralized electricity markets. Due to the excellent breeding capability of the HPTWR, the Th fuel is also added into the breeding fuel region of the reactor to achieve the Th-U fuel cycle in this work.

Methods: The Monte Carlo code RMC is used to obtain the reactivity swing, propagation of axial power peak, burnup, and productions of bred fissile nuclides for the HPTWR with Th and U fuels.

Results and Discussion: The results indicate that the HPTWR with 13.6% ^{235}U enrichment of ignition fuel and 20% ^{235}U enrichment of breeding fuel can continuously operate for 18.1 years without refueling when the mass fraction of ^{232}Th in heavy metals of breeding fuel region is 33%. The propagation velocity of axial power peak and total burnup for the HPTWR with Th and U fuels is about 0.5525 cm/years and 24.72 GWd/THM during the 18.1 years operation respectively. The corresponding productions of bred ^{239}Pu, ^{241}Pu and ^{233}U are about 212.99 kg of ^{239}Pu, 0.19 kg of ^{241}Pu and 81.58 kg of ^{233}U at the end of cycle (EOC) respectively. The obtained results in this study demonstrate that the HPTWR can achieve the Th fuel breeding in the case of the low ^{235}U enrichment loading (≤ 20%).

KEYWORDS

heat pipe, traveling wave reactor, breeding, Monte Carlo code, thorium

1 Introduction

To achieve the sustainable development of nuclear energy, it is necessary to solve the problem of nuclear fuel shortage. As an alternative nuclear fuel resource, thorium is estimated to be 3 to 4 times as abundant in Earth's crust as uranium, with a lower mining cost (Wickleder, 2006). Sustainable supply of nuclear fuel can be achieved by the Th–U fuel cycle, which attracts more and more attention to ensure sustainable energy generation (IAEA-TECDOC-1319, 2002; IAEA-TECDOC-1450, 2005). So, up to now, the Th fuel cycle has been applied to many breeding reactors (Fomin et al., 2011; Zhang et al., 2011; Liem et al., 2016), which show great potential and advantages in realizing efficient utilization of thorium resources.

The micro heat pipe cooled reactor can be applied to the energy systems of decentralized electric markets (such as remote regions, island communities, and military bases) because it has a more compact structure, simple design, safety features, longer lifetime, and higher power output (Yan et al., 2020; Zohuri, 2020). The mass and volume of the designed heat pipe cooled reactor

usually are lighter and smaller, respectively, for better mobility (Wang et al., 2020). Thus, fuel enrichment of the heat pipe cooled reactor is usually much higher than that of the large PWR. The original concepts of heat pipe cooled reactors were pioneered at Los Alamos National Laboratory (LANL) for space applications during the 1960s (Niederauer and Lantz, 1970). In the 21st century, many space heat pipe cooled reactors have been proposed (Sun et al., 2018; Liu et al., 2020; McClure et al., 2020; Zhang et al., 2020; Ma et al., 2021a; Cui et al., 2021; Xiao et al., 2022). In addition, the continual development of heat pipes has led to many research institutes developing high-power heat pipe cooled reactors in decentralized electric markets. Recently, Alawneh et al. (2022) proposed a 3 MW yttrium hydride moderated heat pipe cooled microreactor with UO_2 fuel, which can be operated safely for more than 11 years. LANL (McClure et al., 2015) proposed a 5 MW_{th} heat pipe cooled mobile nuclear reactor (Megapower), which can continuously operate for more than 12 years in the case of 19.75% enriched UO_2 fuel. Guo et al. (2021) analyzed the neutronic characteristics of the Megapower. The results show that the influence of the cross-section library can be >750 pcm and the addition of the axial structure zone can lead to a >300 pcm reactivity increase. Zirconium hydride is introduced in the Meagpower to design a moderated megawatt-class HPR core (Feng et al., 2022). The results show that the moderation of the core can decrease the maximum neutron flux and is beneficial to reducing the thickness and weight of the shield. In addition, many studies (Ma et al., 2020a; Ma et al., 2021b; Ma et al., 2022a; Ma et al., 2022b) focused on thermal-hydraulic analyses of the Megapower. In order to improve the power output of the reactor, Westinghouse Electric Company (2017) proposed a 15 MWe eVinci reactor with UN fuel, which can operate for more than 10 years without refueling. Based on the eVinci-like heat pipe cooled reactor, Hernandez et al. (2019) found that the neutron leakage impact for the small-sized heat pipe reactor is the most limiting factor on the fuel cycle performance. To improve the lifetime of the reactor, the KAIST (Choi et al., 2020) proposed an 18 MW_{th} H-MMR with UN fuel, which provides continuous operation for about 56 years in the case of 12.1% ^{235}U enrichment. In addition, Ehud (2008) proposed a 125 MWth HP-ENHS core, which can achieve at least 20 years of core lifetime by loading the depleted uranium and TRUs.

The neutron breeding wave has been applied in the liquid metal-cooled reactor (Fomin et al., 2011), water-cooled reactor (Zhang et al., 2011), and gas-cooled reactor (Liem et al., 2016), and the breeding of thorium fuel has been achieved in those reactors due to their higher breeding capability. Compared to traditional larger reactors, the heat pipe reactor has a smaller volume of core, and thus, a higher enrichment of fuel is required. Thus, the application of the neutron traveling wave in the heat pipe reactor can reduce the enrichment of fuel and extend the lifetime of the core. The neutron breeding traveling wave has been applied in the heat pipe cooled reactor in our previous work (Ma and Hu, 2022). Figure 1 shows the burnup strategy of the heat pipe cooled traveling wave reactor (HPTWR) power source, which consists of a reactor, shield, and heat exchanger. In the HPTWR, the channels of cooling are inserted into the heat pipe. The fission heat of the reactor is transferred to the heat exchanger by the heat pipe. In the beginning cycle, the reactor usually consists of an ignition fuel region (burnup region) and a breeding fuel region. In the depletion process, the burnup region is transformed axially, in wave form, through the reactor length. The proposed heat pipe cooled traveling wave reactor (HPTWR) consists of an ignition fuel region with 14% ^{235}U enrichment and a

breeding fuel region with 8.5% ^{235}U enrichment, which can continuously operate for 59 years with a 1.2% variation range of k_{eff} in the case of U–Pu fuel cycle. Due to its high breeding capability, the breeding of Th fuel is also explored in the HPTWR. However, the more neutrons will be consumed for the ^{232}Th breeding in the reactor relative to the ^{238}U breeding because it has a longer breeding chain of Th–U. Therefore, ^{232}Th is loaded into the breeding fuel region, and the ^{235}U enrichment of the breeding fuel must not be higher than 20% due to non-proliferation and safeguards. In addition, based on the HPTWR with only U fuel, a part of U fuel must be loaded into the breeding fuel to compensate for the reactivity and achieve the axial propagation of the neutron breeding wave. Section 2 will describe the reactor model. Section 3 will discuss the main burnup results of this model, including the reactivity, axial power distribution, burnup, and breeding capability of the Th–U fuel cycle. Finally, Section 4 will present the conclusion of this paper.

2 Model description

The HPTWR is a heat pipe cooled reactor with 65.5 MW_{th}, which has a total of 1,008 heat pipe fuel elements with ignition and breeding fuel regions (Ma and Hu, 2022). A central heat pipe in each fuel element is surrounded by a uranium nitride (UN) fuel pellet with cladding on both radial sides of the pellet (inner and outer claddings) (Sterbentz et al., 2018). Lithium heat pipes with a radius of 0.71 cm are used for the reactor cooling, where the ^{7}Li enrichment and Li density are 99.9% and 0.414 g/cm^3, respectively (Sun et al., 2018). Figure 2 shows the cross-sections of the fuel element (a) and heat pipe (b). Both the operation temperatures of UN fuel and Li heat pipe in the neutroncis calculation are set to 1,600 K. The Li heat pipe can be replaced during long-term continuous reactor operation due to its high-temperature life limit (Rosenfeld et al., 2004; Choi et al., 2020). The 1,008 fuel elements are surrounded by the axial and radius reflectors to keep the criticality of the reactor. A shutdown/safety rod is located at the center of the reactor. The schematic arrangement and main parameters of the HPTWR are shown in Figure 3 and Table 1, respectively.

All the computational results are performed by the Monte Carlo program RMC (Reactor Monte Carlo code), which is a 3D stochastic neutron transport simulation developed by Tsinghua University (Wang et al., 2015; Ma et al., 2019). The continuous-energy cross-section based on the ENDF/B-VII library is used for the different materials in this study (Chadwick et al., 2006). The calculations of fuel depletion in the HPTWR are based on using 15,000 particles per cycle, with 50 inactive cycles and 200 active cycles (computational uncertainty of less than 30 pcm). In order to simulate the neutron breeding wave of the reactor, the core is divided into 18 smaller zones axially, and each zone is 5 cm long in the axial direction (Shrestha and Rizwan-uddin, 2014; Huang et al., 2015).

3 Results and discussion

3.1 Core lifetime

Owing to the larger neutron capture cross-section (0.15 b at 0.3 MeV) of ^{232}Th compared with its fission cross-section (7.2×10^{-7} b at 0.3 MeV), some enriched ^{235}U fuel is required to maintain the
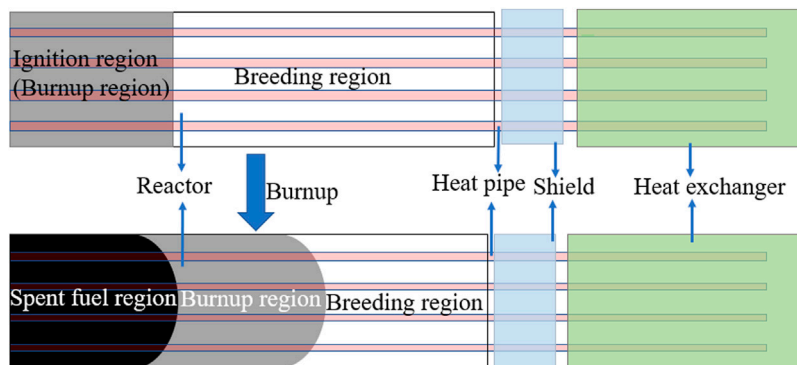
FIGURE 1
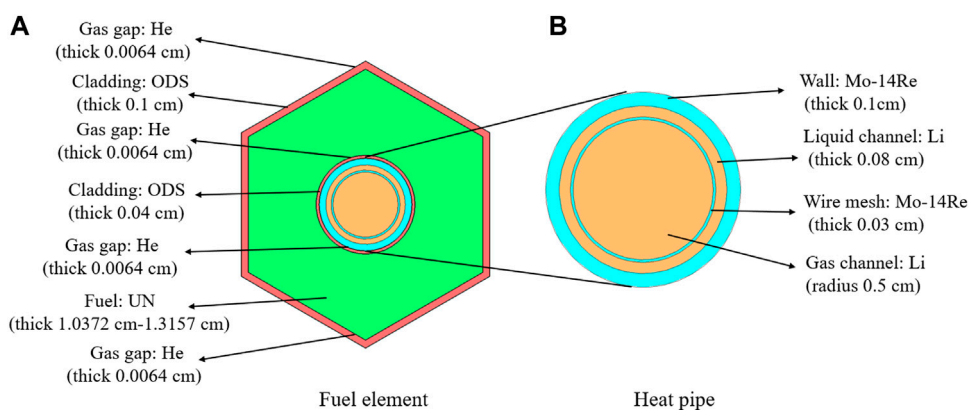Burnup strategy of the heat pipe cooled traveling wave reactor.

FIGURE 2
Cross-sections of the fuel element **(A)** and heat pipe **(B)**.

reactor criticality in the breeding fuel region during the reactor operation. In order to achieve the breeding of Th fuel, U fuel with 20% enrichment of ^{235}U is adopted in the breeding fuel region because of non-proliferation and safeguards. Therefore, both the enrichment of ^{235}U in the ignition fuel region and the mass fraction of Th fuel in the breeding fuel region require to be adjusted to achieve propagation of the neutron traveling wave. Table 2 shows three scenarios to study the effect of the loaded ^{232}Th amount on the reactor reactivity. Figure 4 shows the k_{eff} of the reactor for three scenarios during the operation. The three scenarios have the same initial k_{eff} (about 1.002). The k_{eff} for scenarios 2 and 3 gradually increase during the first 25 years because the bred fissile ^{239}Pu and ^{241}Pu in the reactor provide a higher positive reactivity. Then, the k_{eff} gradually decreases during the next operation time because a large number of nuclear fuel gets consumed in the reactor. The k_{eff} for scenario 1 gradually decreases during the whole operation because it is loaded into a large number of ^{232}Th in the breeding fuel region. It can be seen that the lifetime of scenarios 1, 2, and 3 are about 11.3 years, 18.1 years, and 18.8 years, respectively, and the corresponding k_{eff} ranges of variation (swing) remain about 0.2%,

0.35%, and 0.4%, respectively. The breeding chain of the Th–U fuel cycle is longer than that of the U–Pu fuel cycle, and the half-life of ^{233}Pa (about 27 days) produced by the neutron capture and the decay of ^{232}Th is longer than that of ^{239}U (about 23 min) produced by the neutron capture of ^{238}U (Jiang et al., 2012). Therefore, the consumed fission neutron amount for the ^{232}Th breeding is higher than that for the ^{238}U breeding, which decreases the lifetime of the HPTWR with only U fuel (about 59 years).

In order to investigate the propagation of neutron breeding wave, Figure 5 shows the spacial and temporal profiles of axial power density distributions for scenarios 1, 2, and 3. The power density peak for scenario 1 is always in the ignition fuel region during the whole operation because it has a shorter lifetime of the reactor. The power density peak for scenario 3 is in the breeding fuel region at the BOC because the ignition and breeding fuel regions have lower and higher ^{235}U enrichments, respectively. In addition, the axial power density peak is always in the 47.5 cm axial position during the whole operation, which has the higher radiation damage for the structural materials in the 47.5 cm axial position. In addition, higher Th fuel loading can achieve a higher ^{233}U production rate in the reactor,
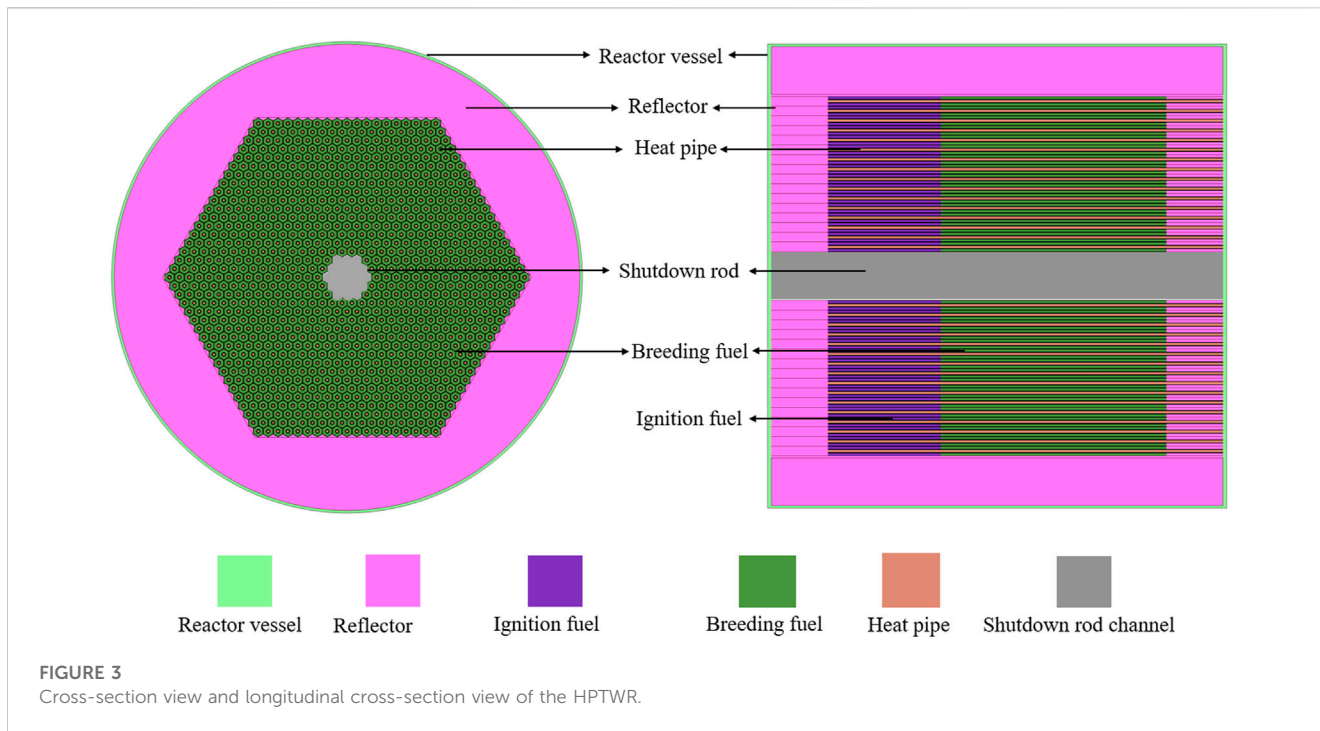
FIGURE 3
Cross-section view and longitudinal cross-section view of the HPTWR.

TABLE 1 Main parameters for the HPTWR with Th and U fuels.

Parameters	Value	Parameters	Value
Power (MW$_{th}$)	65.5	Heat pipe wall material	Mo-14Re
Total number of heat pipes	1,008	Density of Mo-14Re (g/cm^3)	12
Fuel	UN	Wick material	Mo-14Re
^{15}N enrichment in fuel (%)	99.9	Heat pipe outer radius (cm)	0.71
Density of fuel (g/cm^3)	13.59	Heat pipe wall thickness (cm)	0.1
^{235}U enrichment of ignition fuel (wt%)	13.6	Liquid lithium channel thickness (cm)	0.08
^{235}U enrichment of breeding fuel (wt%)	20	Wick thickness (cm)	0.03
Mass fraction of ^{232}Th in heavy metals of breeding fuel region	33%	Gas lithium channel radius (cm)	0.5
Ignition region length (cm)	30	Reflector material	Al$_2$O$_3$
Breeding region length (cm)	60	Density of reflector (g/cm^3)	3.9
Mass of heavy metal (t)	10.90	Temperature of reflector (K)	900
Element to element pitch (cm)	3.8256	Side reflector outer radius (cm)	77.8
Fuel cladding material	Mo-14Re	Radial reflector thickness (cm)	18.71–28.30
Outer cladding thickness (cm)	0.1	Axial reflector length (cm)	15
Inner cladding thickness (cm)	0.04	Safety rod channel outer radius (cm)	8

which has been shown in our previous works (Ma et al., 2020b; Ma et al., 2020c). Therefore, scenario 2 is recommended for ^{232}Th fuel breeding in the HPTWR.

For scenario 2, the ignition fuel region has the higher power distribution relative to the breeding fuel region at the beginning of cycle (BOC) because the ignition fuel region has the higher ^{235}U fuel density. The total power density of ignition and breeding fuel regions are about 527.12 MW$_{th}$/m^3 and 855.2 MW$_{th}$/m^3 at the BOC, respectively. The power distributions in the ignition and breeding fuel regions continuously decrease and increase during the reactor operation, respectively, because many ^{235}U are consumed in the ignition fuel region, and many new fissile nuclides are bred in

TABLE 2 Th and U breeding scenarios under different conditions.

	Ignition fuel	Breeding fuel	
Scenario	^{235}U enrichment (%)	^{235}U enrichment (%)	^{232}Th mass fraction in heavy metals (%)
1	14.23	20	35
2	13.6	20	33
3	11.9	20	30
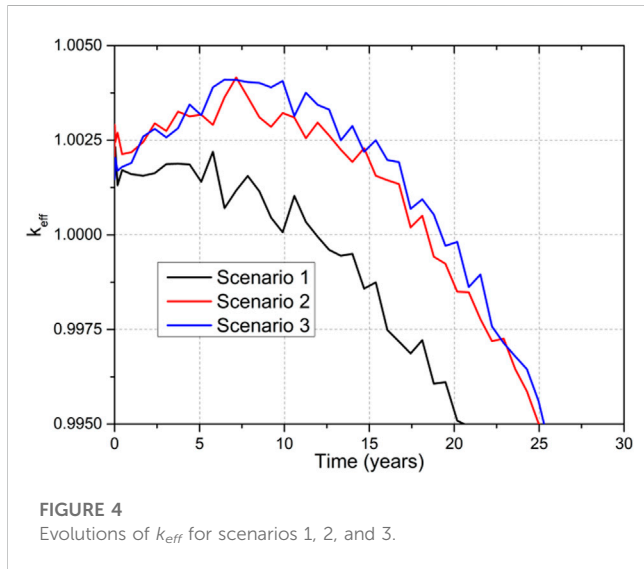
FIGURE 4
Evolutions of k_{eff} for scenarios 1, 2, and 3.

FIGURE 5
Axial power profiles of scenarios 2 **(A)**, 1 and 3 **(B)**.

the breeding fuel region. It can also be seen that the axial position of the power peak has been shifted to the breeding fuel region at the end of cycle (EOC). The axial power density peak is decreased from about 103.21 MW$_{th}$/m^3 at the BOC to about 96.45 MW$_{th}$/m^3 at the EOC due to the flattening of axial power distribution. The axial peak locations of power distribution at the BOC and EOC are about 27.5 and 37.5 cm in Figure 5, respectively. The resulting traveling wave speed is about 0.5525 cm/year, which is higher than that of the U–Pu fuel cycle (0.5085 cm/year) because the ^{235}U mass densities between the ignition fuel region and breeding fuel region have a relatively smaller difference.

The shift of the axial power peak has a significant influence on the local burnup of scenario 2 during the reactor operation. The core was divided into six subregions to analyze the local burnup of fuel, which is shown in Table 3. Figure 6 shows the burnups for subregions of scenario 2 during the 18.1 years of operation. Subregions 2 and 3 have higher burnup rates because they have higher local powers during operation. Subregions 5 and 6 have lower burnups of fuel because the axial power peak is only shifted to subregion 3 at the EOC. The burnups for subregions 1, 2, 3, 4, 5, and 6 are increased to about 38.07 GWd/THM, 50.50 GWd/THM, 51.49 GWd/THM, 46.76 GWd/THM, 36.83 GWd/THM, and 23.79 GWd/THM, respectively, at the EOC. In addition, the burnups per small zones at the EOC are shown in Figure 7. The maximum burnup of small zones in the ignition fuel region is about 52.84 GWd/THM at the EOC, whose corresponding axial position is 27.5 cm because it has the highest power value during the whole reactor operation. The maximum burnup of small zones in the breeding fuel
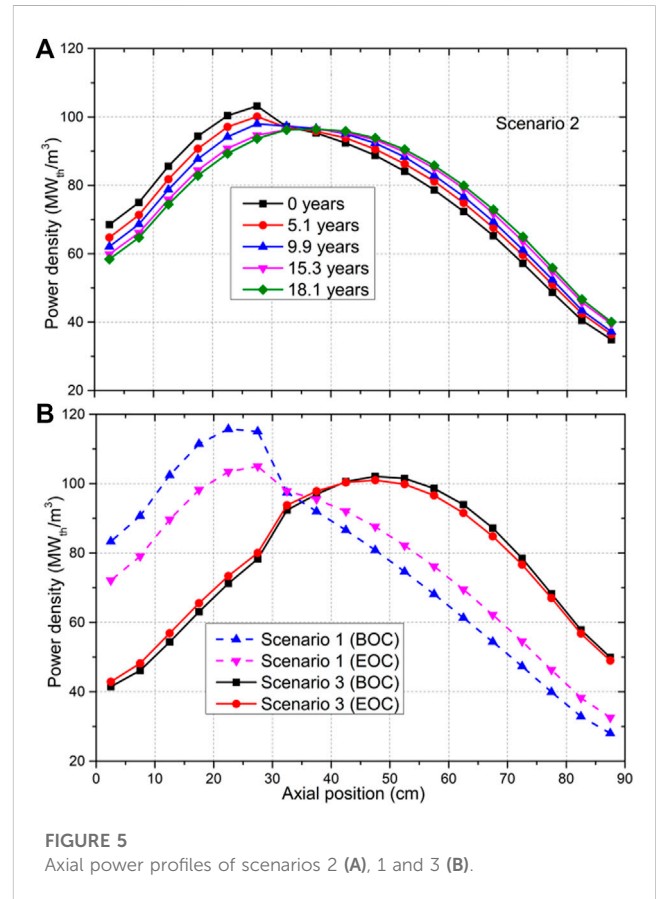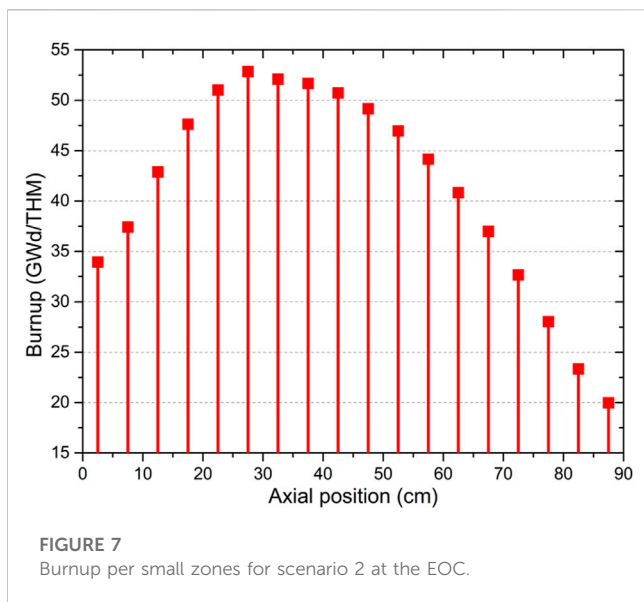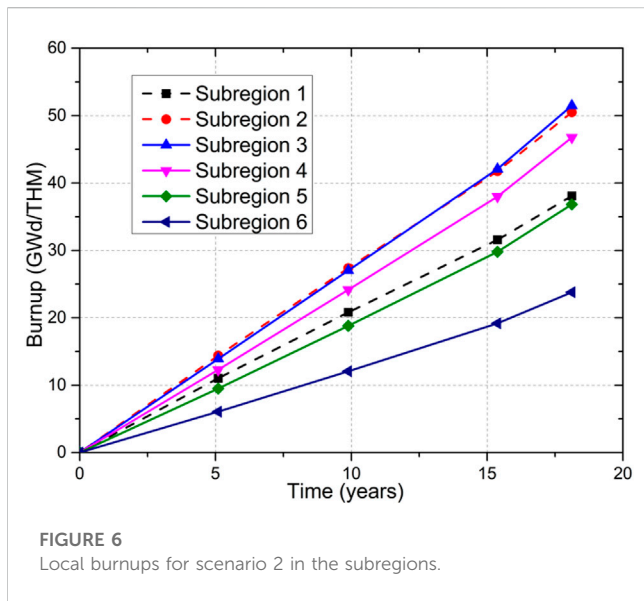
region is about 52.09 GWd/THM at the EOC, whose corresponding axial position is 32.5 cm because its axial position is close to the ignition fuel region and has a relatively higher power value during the whole reactor operation. The minimum burnups of small zones in the ignition and breeding fuel regions are about 33.93 GWd/THM and 19.99 GWd/THM, respectively, whose axial positions are 2.5 and 87.5 cm, respectively, because their axial positions are close to the axial reflector and have relatively lower power value during the whole reactor operation. The total burnup for the HPTWR with Th and U fuels is about 24.72 GWd/THM at 18.1 years.
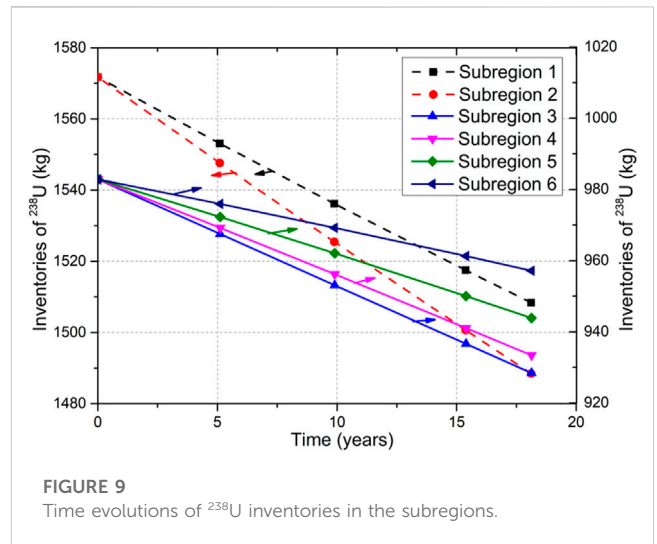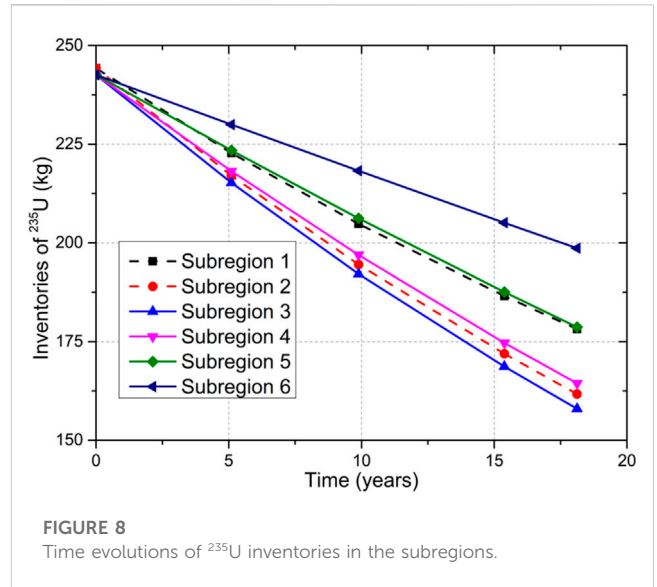
3.2 Breeding capability

The continuous operation time of the HPTWR with Th and U fuels is about 18.1 years, which is about 40.9 years less than that with only U fuel (about 59 years). Thus, the nuclear fuel consumption

TABLE 3 Designation of subregions for the HPTWR with Th and U fuels.

Zones	Subregion
1–3	1 (Ignition region)
3–6	2 (Ignition region)
6–9	3 (Breeding region)
9–12	4 (Breeding region)
13–15	5 (Breeding region)
15–18	6 (Breeding region)

FIGURE 6
Local burnups for scenario 2 in the subregions.

FIGURE 7
Burnup per small zones for scenario 2 at the EOC.

FIGURE 8
Time evolutions of ^{235}U inventories in the subregions.

FIGURE 9
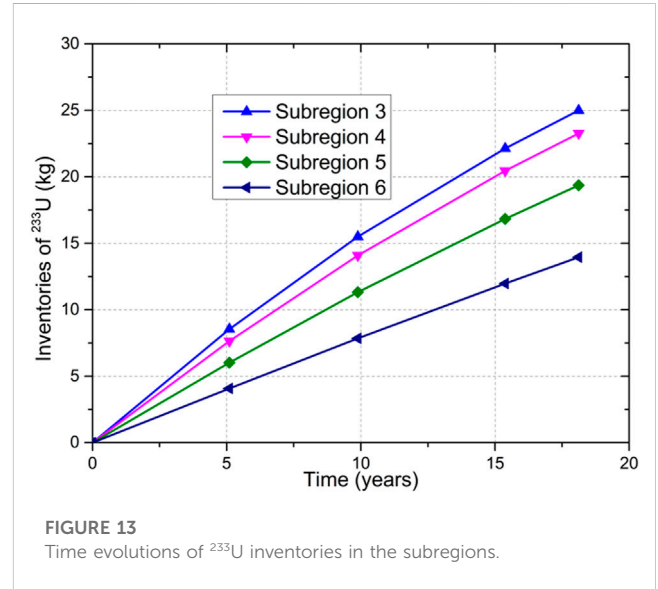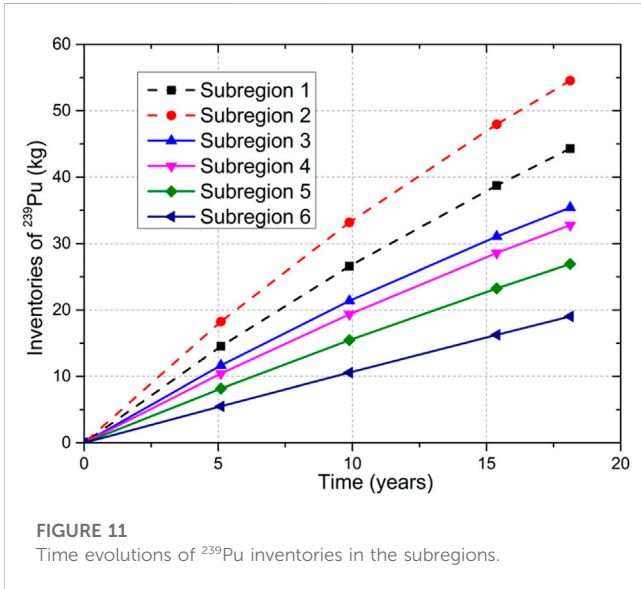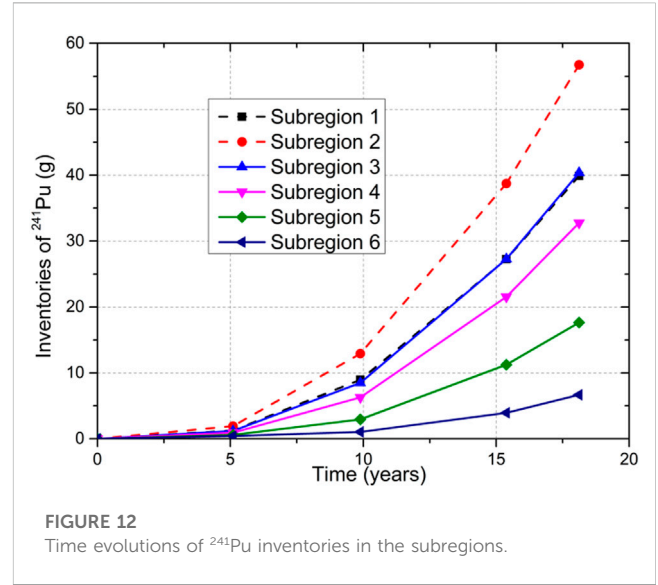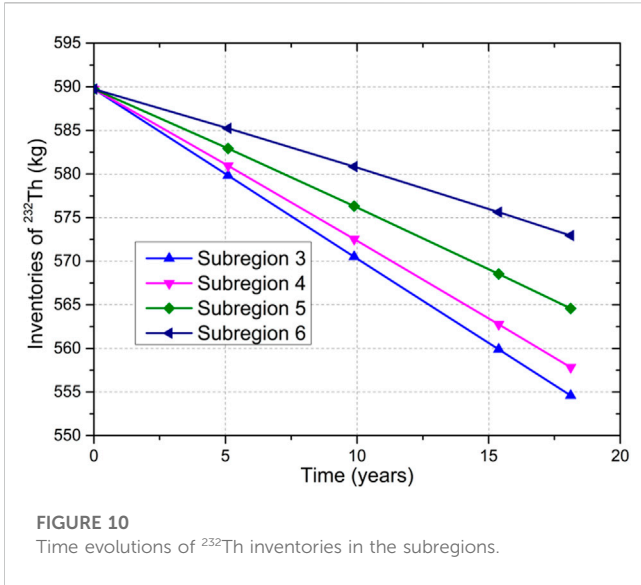Time evolutions of ^{238}U inventories in the subregions.

amount and Th–U breeding capability of the HPTWR will be evaluated during the reactor operation. In order to investigate the amount of consumed nuclear fuel, Figures 8–10 show the inventories of ^{235}U, ^{238}U, and ^{232}Th in the six subregions of the HPTWR with Th and U fuels, respectively. Figures 11–13 show the inventories of the main bred fissile nuclides in the six subregions of the reactor.

The reactivity of the core mainly comes from the fission reaction of ^{235}U at the early operation of the core since the newly produced fissile nuclides are smaller in the reactor. The inventories of ^{235}U in subregions 2 and 3 have faster consumption rates in the ignition and breeding regions during the operation, respectively, because they have higher local powers. In addition, subregion 6 has the highest ^{235}U inventory at the EOC due to its lowest power during the whole operation. The inventories of ^{235}U in subregions 1 and 2 are decreased from 244.28 kg to about 178.18 and 161.72 kg, respectively, and the decreased amounts are about 66.1 and 82.56 kg, respectively. The inventories of ^{235}U in subregions 3, 4, 5, and 6 are about 157.98, 164.4, 178.68, and 198.63 kg, respectively, at the EOC, and the corresponding decreased amounts are about

FIGURE 10
Time evolutions of ^{232}Th inventories in the subregions.

FIGURE 12
Time evolutions of ^{241}Pu inventories in the subregions.

FIGURE 11
Time evolutions of ^{239}Pu inventories in the subregions.

FIGURE 13
Time evolutions of ^{233}U inventories in the subregions.

84.61, 78.19, 63.91, and 43.96 kg, respectively (242.59 kg at BOC). The higher local power has a higher neutron flux in the HPTWR. Therefore, more ^{238}U and ^{232}Th will be transformed into ^{239}Pu and ^{233}U in the higher local power position of the HPTWR, respectively. The ^{238}U inventories in subregions 1 and 2 have higher consumption rates because they have higher initial ^{238}U loading inventories. The inventories of ^{238}U in subregions 1 and 2 are decreased from about 1571.74 kg at the BOC to about 1508.35 kg and 1488.48 kg at the EOC, respectively, and the corresponding decreased amounts are about 63.39 and 83.26 kg, respectively. The consumption rates of ^{238}U for subregions 3, 4, 5, and 6 sequentially decrease during operation due to their decrease of power distribution. The amounts of consumed ^{238}U in subregions 3, 4, 5, and 6 are about 54.38, 49.37, 38.93, 25.64, and 85.97 kg, respectively, during the 18.1 years of operation. Similar to ^{238}U inventories in the breeding fuel region, the amounts of consumed ^{232}Th in subregions 3, 4, 5, and

6 are about 35.14, 31.9, 25.17, and 16.80 kg, respectively, during the 18.1 years of operation (from about 589.74 kg to about 554.60, 557.84, 564.58, and 572.94 kg, respectively).

The breeding capability of the HPTWR can be evaluated by the productions of the newly produced fissile nuclides. The produced fissile nuclides in the U–Pu fuel cycle and Th–U fuel cycle consist of Pu isotopes (^{239}Pu and ^{241}Pu) and U isotope (^{233}U) in the traveling wave reactor, respectively. Figures 11–13 show the main inventories of produced fissile nuclides (^{239}Pu, ^{241}Pu, and ^{233}U). The bred ^{239}Pu inventories in subregions 1 and 2 are higher than those in subregions 3, 4, 5, and 6 because they have higher initial ^{238}U loading inventories. The productions of ^{239}Pu for subregions 3, 4, 5, and 6 sequentially decrease during the operation due to their decrease of power distribution. The productions of accumulated ^{239}Pu in subregions 1, 2, 3, 4, 5, and 6 are about 44.29, 54.54, 35.41, 32.78, 26.93, and 19.03 kg at

FIGURE 14
Productions of ^{239}Pu, ^{241}Pu, and ^{233}U per small zones at the EOC.

FIGURE 15
Consumed nuclear fuel amounts and produced fissile nuclide amounts in the HPTWR with two fuel loading scenarios.
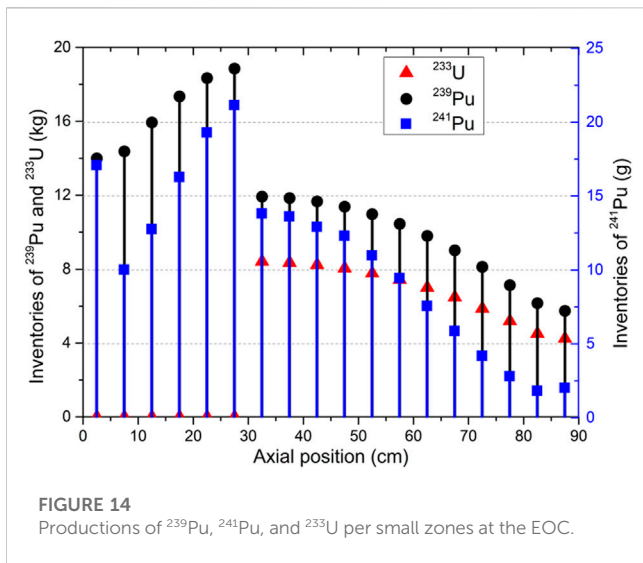
the EOC, respectively. The corresponding productions of accumulated ^{241}Pu in subregions 1, 2, 3, 4, 5, and 6 are about 39.89, 56.75, 40.35, 32.75, 17.64, and 6.67 g at the EOC, respectively. The inventories of ^{241}Pu in the HPTWR are much less than those of ^{239}Pu because ^{241}Pu is produced by the sequence neutron captures of ^{239}Pu in the depletion process. The total productions of ^{239}Pu and ^{241}Pu in the HPTWR with U and Th fuels are about 212.99 kg and 194.05 g, respectively. In addition, the productions of accumulated ^{233}U in subregions 3, 4, 5, and 6 are about 25.00, 23.27, 19.36, and 13.94 kg at the EOC, respectively, and the total production of ^{233}U is about 81.58 kg.

The corresponding produced fissile nuclides per small zones of the HPTWR with U and Th fuels at the EOC are shown in Figure 14. The ^{239}Pu productions per small zones in the ignition fuel region are higher than those in the breeding fuel region at the EOC because it has a higher neutron flux, and more ^{238}U will be transformed into ^{239}Pu during the whole reactor operation. The highest ^{239}Pu production of small zones in the ignition fuel region is about 18.85 kg, whose axial position is 27.5 cm because it always has a relatively higher neutron flux during the reactor operation. Similar to ^{239}Pu production, the highest ^{241}Pu production of small zones in the ignition fuel region is about 21.15 g at the EOC in the axial position of 27.5 cm. It can be seen that the ^{241}Pu production of small zones in the 2.5 cm axial position (17.09 g) is also higher than that in the 7.5 cm axial position (10.04 g) because more thermal neutrons will be reflected from the reflector in the 2.5 cm axial position and ^{239}Pu has a much higher thermal neutron capture cross-section (about 271.0 b at 0.0253 MeV) relative to ^{238}U (about 8.4 b at 0.0253 MeV). The ^{233}U productions of small zones in the ignition fuel region are 0 kg because no ^{232}Th is loaded into the ignition fuel region. The productions of small zones for ^{239}Pu, ^{241}Pu, and ^{233}U in the breeding fuel region gradually decrease with the increase of axial position because of the decrease of power and neutron flux of small zones. The lowest productions of small zones for ^{239}Pu, ^{241}Pu, and ^{233}U are about 5.74 kg, 2.02 g, and 4.24 kg in the breeding fuel region, whose axial position is at 87.5 cm.
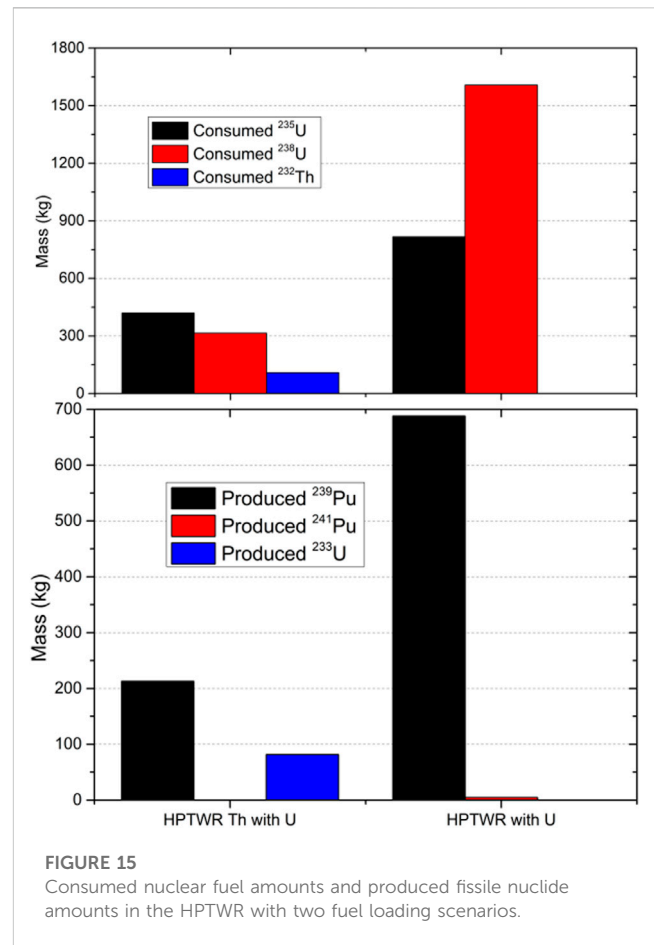
The lifetime of the HPTWR with Th and U fuels is decreased by about 40.9 years relative to the HPTWR with only U fuel. In order to investigate the amounts of consumed nuclear fuel and produced fissile nuclides, Figure 15 shows the consumed U and Th amounts and produced ^{239}Pu, ^{241}Pu, and ^{233}U amounts in the HPTWR with two fuel loading scenarios during the whole operation. The total amount of produced fissile Pu isotopes in the HPTWR with Th and U fuels during the 18.1 years of operation (about 212.99 kg of ^{239}Pu and 0.19 kg of ^{241}Pu) is 479.79 kg less than that in the HPTWR with only U fuel during the 59 years of operation (about 688.11 kg of ^{239}Pu and 4.86 kg of ^{241}Pu). However, the total amount of consumed U isotopes in the HPTWR with Th and U fuels (419.32 kg of ^{235}U and 314.98 kg of ^{238}U) during the 18.1 years of operation is about 1689.37 kg less than that in the HPTWR with only U fuel during the 59 years of operation (816.46 kg of ^{235}U and 1607.21 kg of ^{238}U). In addition, the HPTWR with Th and U fuels can consume about 109.01 kg of ^{232}Th and produce about 81.58 kg of ^{233}U.

4 Conclusion

In this work, the breeding capability and nuclear fuel consumption for a heat pipe cooled traveling wave reactor with Th and U fuels were investigated using the RMC code. The lifetime, propagation velocity of axial power peak, burnup, consumption of

nuclear fuel, and breeding capability of the reactor are discussed. The conclusion obtained can be summarized as follows:

1. The HPTWR loaded with 13.6% ^{235}U enrichment of ignition fuel and 20% ^{235}U enrichment of breeding fuel can continuously operate for about 18.1 years without refueling when the mass fraction of ^{232}Th in the heavy metals of the breeding fuel region is about 33%. The range of variation (swing) of k_{eff} remains within 0.35% during the 18.1 years of operation. The results indicate that the HPTWR can achieve utilization of Th fuel for better economy and sustainability.
2. The propagation velocity of the axial power peak and burnup for the HPTWR with Th and U fuels are about 0.5525 cm/years and 24.72 GWd/THM during the 18.1 years of operation, respectively. The burnup in the ignition fuel region is higher than that in the breeding fuel region at the EOC.
3. The HPTWR with Th and U fuels can produce about 212.99 kg of ^{239}Pu, 0.19 kg of ^{241}Pu, and 81.58 kg of ^{233}U at 18.1 years. The productions of ^{239}Pu and ^{241}Pu in the ignition fuel region are higher than those in the breeding fuel region at the EOC, and the productions of bred fissile nuclides (^{239}Pu, ^{241}Pu, and ^{233}U) in the breeding fuel region gradually decrease with the increase of the axial position of the reactor.

Data availability statement

The raw data supporting the conclusion of this article will be made available by the authors, without undue reservation.

Author contributions

PH and KM contributed to the conception and design of the study. KM performed the numerical analysis and wrote the first draft of the manuscript. All authors contributed to manuscript revision and read and approved the submitted version.

Funding

Conflict of interest

The authors declare that the research was conducted in the absence of any commercial or financial relationships that could be construed as a potential conflict of interest.

Publisher's note

All claims expressed in this article are solely those of the authors and do not necessarily represent those of their affiliated organizations, or those of the publisher, the editors, and the reviewers. Any product that may be evaluated in this article, or claim that may be made by its manufacturer, is not guaranteed or endorsed by the publisher.

References

Alawneh, L. M., Vaghetto, R., Hassan, Y., and White, H. G. S. (2022). Conceptual design of a 3 MWth yttrium hydride moderated heat pipe cooled micro reactor. *Nucl. Eng. Des.* 397, 111931. doi:10.1016/j.nucengdes.2022.111931

Chadwick, M. B., Obložinský, P., Herman, M., Greene, N., McKnight, R., Smith, D., et al. (2006). ENDF/B-VII.0: Next generation evaluated nuclear data library for nuclear science and technology. *Nucl. data sheets* 107, 2931–3060. doi:10.1016/j.nds.2006.11.001

Choi, Y. J., Lee, S., Jang, S., Son, I. W., Kim, Y., et al. (2020). Conceptual design of reactor system for hybrid micro modular reactor (H-MMR) using potassium heat pipe. *Nucl. Eng. Des.* 370, 110886. doi:10.1016/j.nucengdes.2020.110886

Cui, D., Dai, Y., Cai, X., Fu, Y., Li, X., Zou, Y., et al. (2021). Preconceptual nuclear design of a 50 kWth heat pipe cooled micro molten salt reactor (micro-MSR). *Prog. Nucl. Energy* 134, 103670. doi:10.1016/j.pnucene.2021.103670

Ehud, G. (2008). Solid-core heat-pipe nuclear battery type reactor. Report No.: DE-FC07-05ID14706. Available at: https://www.osti.gov/servlets/purl/940911 (Accessed September 30, 2008).

Feng, K., Wu, Y., Hu, J., Jin, X., Gu, H., and Guo, H. (2022). Preliminary analysis of a zirconium hydride moderated megawatt heat pipe reactor. *Nucl. Eng. Des.* 388, 111622. doi:10.1016/j.nucengdes.2021.111622

Fomin, S. P., Fomin, O. S., Mel'nik, Yu.P., Pilipenko, V., and Shul'ga, N. (2011). Nuclear burning wave in fast reactor with mixed Th-U fuel. *Prog. Nucl. Energ* 53, 800–805. doi:10.1016/j.pnucene.2011.05.004

Guo, H., Feng, K., Gu, H., Yao, X., and Bo, L. (2021). Neutronic modeling of megawatt-class heat pipe reactors. *Ann. Nucl. Energy* 154, 108140. doi:10.1016/j.anucene.2021.108140

Hernandez, R., Todosow, M., and Brown, N. R. (2019). Micro heat pipe nuclear reactor concepts: Analysis of fuel cycle performance and environmental impacts. *Ann. Nucl. Energy* 126, 419–426. doi:10.1016/j.anucene.2018.11.050

Huang, J. F., Han, J. L., Cai, X. Z., Ma, Y., Li, X., Zou, C., et al. (2015). Breed-and-burn strategy in a fast reactor with optimized starter fuel. *Prog. Nucl. Energy* 85, 11–16. doi:10.1016/j.pnucene.2015.05.007

IAEA-TECDOC-1319 (2002). *Thorium fuel utilization: Options and trends.* Vienna, Austria: IAEA.

IAEA-TECDOC-1450 (2005). *Thorium fuel cycle-potential benefits and challenges.* Vienna, Austria: IAEA.

Jiang, M., Xu, H., and Dai, Z. (2012). Advanced fission energy program-TMSR nuclear energy system. *Bull. Chin. Acad. Sci.* 27 (3).

Liem, P. H., Tran, H. N., and Sekimoto, H. (2016). Burnup performance of small-sized long-life CANDLE high temperature gas-cooled reactors with U–Th–Pa fuel. *Ann. Nucl. Energy* 91, 36–47. doi:10.1016/j.anucene.2016.01.001

Liu, X., Zhang, R., Liang, L., Tang, S., Wang, C., Tian, W., et al. (2020). Core thermal-hydraulic evaluation of a heat pipe cooled nuclear reactor. *Ann. Nucl. Energy* 142, 107412. doi:10.1016/j.anucene.2020.107412

Ma, K., and Hu, P. (2022). Preliminary conceptual design and neutroncis analysis of a heat pipe cooled traveling wave reactor. *Ann. Nucl. Energy* 168, 108907. doi:10.1016/j.anucene.2021.108907

Ma, K., Yu, C., Cai, X., Zou, C. Y., and Chen, J. G. (2020). Transmutation of ^{129}I in a single-fluid double-zone thorium molten salt reactor. *Nucl. Sci. Tech.* 31 (1), 10. doi:10.1007/s41365-019-0720-1

Ma, K., Yu, C., Chen, J., and Cai, X. (2020). Transmutation of ^{135}Cs in a single-fluid double-zone thorium molten salt reactor. *Int. J. Energy Res.* 45, 12203–12214. doi:10.1002/er.6235

Ma, Y., Chen, E., Yu, H., Zhong, R., Deng, J., Chai, X., et al. (2020). Heat pipe failure accident analysis in megawatt heat pipe cooled reactor. *Ann. Nucl. Energy* 149, 107755. doi:10.1016/j.anucene.2020.107755

Ma, Y. G., Liu, S. C., Luo, Z., Huang, S., Li, K., Wang, K., et al. (2019). RMC/CTF multiphysics solutions to VERA core physics benchmark problem 9. *Ann. Nucl. Energy* 133, 837–852. doi:10.1016/j.anucene.2019.07.033

Ma, Y., Han, W., Xie, B., Yu, H., Liu, M., He, X., et al. (2021). Coupled neutronic, thermal-mechanical and heat pipe analysis of a heat pipe cooled reactor. *Nucl. Eng. Des.* 384, 111473. doi:10.1016/j.nucengdes.2021.111473

Ma, Y., Liu, J., Yu, H., Tian, C., Huang, S., Deng, J., et al. (2022). Coupled irradiation-thermal-mechanical analysis of the solid-state core in a heat pipe cooled reactor. *Nucl. Eng. Technol.* 54, 2094–2106. doi:10.1016/j.net.2022.01.002

Ma, Y., Tian, C., Yu, H., Zhong, R., Zhang, Z., Huang, S., et al. (2021). Transient heat pipe failure accident analysis of a megawatt heat pipe cooled reactor. *Prog. Nucl. Energy.* 140, 103904. doi:10.1016/j.pnucene.2021.103904

Ma, Y., Zhong, R., Yu, H., Huang, S., Tian, C., He, X., et al. (2022). Startup analyses of a megawatt heat pipe cooled reactor. *Prog. Nucl. Energy.* 153, 104405. doi:10.1016/j.pnucene.2022.104405

McClure, P., Poston, D., Rao, D. V., and Stowers, R. R. (2015). "Design of megawatt power level heat pipe reactors,". Report No.: LA-UR-15-28840. Available at: https://www.osti.gov/biblio/1226133 (Accessed November 12, 2015).

McClure, P. R., Poston, D. I., Gibson, M. A., Mason, L. S., and Robinson, R. C. (2020). Kilopower project: The KRUSTY fission power experiment and potential missions. *Nucl. Technol.* 206, 1–12. doi:10.1080/00295450.2020.1722554

Niederauer, G., and Lantz, E. (1970). "A split-core heat-pipe reactor for space power applications,". Report No.: NASA TM X-52918. Available at: https://www.osti.gov/biblio/7366283 (Accessed January 1, 1970).

Rosenfeld, J. H., Ernst, D. M., Lindemuth, J. E., and Sanzi, J. L. (2004). "An overview of long duration sodium heat pipe tests,". Report No.: NASA/TM-2004-212959. Available at: https://ntrs.nasa.gov/api/citations/20130013063/downloads/20130013063.pdf (Accessed February 8-12, 2004).

Shrestha, R., and Rizwan-uddin (2014). Modeling space-time evolution of flux in a traveling wave reactor. *Ann. Nucl. Energy* 70, 90–95. doi:10.1016/j.anucene.2014.03.011

Sterbentz, J. W., Werner, J. E., Hummel, A. J., Kennedy, J. C., O'Brien, R. C., Dion, A. M., et al. (2018). *Preliminary assessment of two alternative core design concepts for the special purpose reactor*. Idaho Falls, ID, USA: Idaho National Lab. INL.

Sun, H., Wang, C. L., Ma, P., Liu, X., Tian, W., Qiu, S., et al. (2018). Conceptual design and analysis of a multipurpose micro nuclear reactor power source. *Ann. Nucl. Energy* 121, 118–127. doi:10.1016/j.anucene.2018.07.025

Wang, D. Q., Yan, B. H., and Chen, J. Y. (2020). The opportunities and challenges of micro heat piped cooled reactor system with high efficiency energy conversion units. *Ann. Nucl. Energy* 149, 107808. doi:10.1016/j.anucene.2020.107808

Wang, K., Li, Z. G., She, D., Liang, J., Xu, Q., Qiu, Y., et al. (2015). RMC- A Monte Carlo code for reactor core analysis. *Ann. Nucl. Energy* 82, 121–129. doi:10.1016/j.anucene.2014.08.048

Westinghouse Electric Company, 2017. Westinghouse EVinci TM Reactor for Off-Grid Markets. Available at: https://www.researchgate.net/publication/329086061_Westinghouse_eVinciTM_Reactor_for_off-Grid_Markets. (Accessed July 2018).

Wickleder, M. S. (2006). "Thorium," in *The chemistry of the actinide and transactinide elements* (Berlin, Germany: Springer), 52.

Xiao, W., Li, X., Li, P., Zhang, T., and Liu, X. (2022). High-fidelity multi-physics coupling study on advanced heat pipe reactor. *Comput. Phys. Commun.* 270, 108152. doi:10.1016/j.cpc.2021.108152

Yan, B. H., Wang, C., and Li, L. G. (2020). The technology of micro heat pipe cooled reactor: A review. *Ann. Nucl. Energy* 135, 106948. doi:10.1016/j.anucene.2019.106948

Zhang, D. L., Chen, X. N., Gabrielli, F., Rineiski, A., Maschek, W., and Schulenberg, T. (2011). Numerical studies of nuclear traveling waves in a supercritical water cooled fast reactor. *Prog. Nucl. Energy* 53, 806–813. doi:10.1016/j.pnucene.2011.05.027

Zhang, W. W., Zhang, D. L., Wang, C. L., Tian, W., Qiu, S., and Su, G. (2020). Conceptual design and analysis of a megawatt power level heat pipe cooled space reactor power system. *Ann. Nucl. Energy* 144, 107576. doi:10.1016/j.anucene.2020.107576

Zohuri, B. (2020). *Nuclear micro reactors*. Cham Switzerland: Springer International Publishing. doi:10.1007/978-3-030-47225-2